Journal of Geochemical Exploration 199 (2019) 53–59

Contents lists available at ScienceDirect

Journal of Geochemical Exploration

journal homepage: www.elsevier.com/locate/gexplo

Quantification of coffinite ($USiO_4$) in roll-front uranium deposits using visible to near infrared (Vis-NIR) portable field spectroscopy

Benoit Hebert[a], Fabien Baron[b], Valentin Robin[c,*], Karl Lelievre[a], Nicolas Dacheux[d], Stéphanie Szenknect[d], Adel Mesbah[d], Adrien Pouradier[e], Ruslan Jikibayev[e], Régis Roy[f], Daniel Beaufort[a]

[a] Université de Poitiers, CNRS UMR 7285 IC2MP, HydrASA Bât. B35, 6 rue Michel Brunet, 86073 Poitiers Cedex 9, France
[b] Université de Nantes - CNRS UMR 6112 Laboratoire de Planétologie et Géodynamique (LPG), 2 rue de la Houssinière, 44322 Nantes, France
[c] Université de Limoges, Laboratoire Peirene, 123 Avenue A. Thomas, 87060 Limoges Cedex, France
[d] ICSM, CEA, CNRS, ENSCM, Univ Montpellier, Site de Marcoule, Bât. 426, BP 17171, 30207 Bagnols-sur-Cèze, France
[e] KATCO, 282 Ave Dostyk, 050020 Almaty, Kazakhstan
[f] AREVA Resources Canada Inc., P.O. Box 9204, 810 – 45th Street West, Saskatoon, SK S7K 3X5, Canada

ARTICLE INFO

Keywords:
Near infrared
Portable field spectroscopy
Coffinite
Roll-front deposits
Ore exploration
Mineral quantification

ABSTRACT

Coffinite ($USiO_4$) is a common uranium-bearing mineral of roll-front uranium deposits. This mineral can be identified by the visible near infrared (Vis-NIR) portable field spectrometers used in mining exploration. However, due to the low detection limits and associated errors, the quantification of coffinite abundance in the mineralized sandstones or sandy sediments of roll-front uranium deposits using Vis-NIR spectrometry requires a specific methodological development.

In this study, the 1135 nm absorption band area is used to quantify the abundance of coffinite. This absorption feature does not interfere with NIR absorption bands of any other minerals present in natural sands or sandstones of uranium roll-front deposits. The correlation between the 1135 nm band area and coffinite content was determined from a series of spectra measured from prepared mineral mixtures. The samples were prepared with a range of weighted amounts of arenitic sands and synthetic coffinite simulating the range of uranium concentration encountered in roll-front uranium deposits.

The methodology presented in this study provides the quantification of the coffinite content present in sands between 0.03 wt% to 1 wt% coffinite with a detection limit as low as 0.005 wt%. The integrated area of the 1135 nm band is positively correlated with the coffinite content of the sand in this range, showing that the method is efficient to quantify coffinite concentrations typical of roll-front uranium deposits. The regression equation defined in this study was then used as a reference to predict the amount of natural coffinite in a set of mineralized samples from the Tortkuduk uranium roll-front deposit (South Kazakhstan).

1. Introduction

Field-based visible near infrared (Vis-NIR) reflectance spectroscopy has been routinely used in mining exploration for over 30 years. It is a robust and low-cost technique that can be applied in the field to identify minerals with absorption features between 350 and 2500 nm. This technique can also be used to semi-quantify the abundance of the main minerals that are encountered in the alteration halos surrounding the ore deposits. Several publications have discussed the use of Vis-NIR spectroscopy to characterize ore (Ramanaidou et al., 2015; Dill, 2016), to map the distribution of minerals associated with ore deposits through airborne or space-borne hyperspectral sensors (Kruse et al., 2003) and to identify *in situ* gangue minerals and associated alteration halos during mining exploration phases (Hunt and Ashley, 1979; Pontual et al., 1997; Herrmann et al., 2001; Hauff, 2008). This technique has been recently used for the exploration of volcanic-type uranium deposits (Xu et al., 2017) and unconformity-type uranium deposits (Mathieu et al., 2017). In both cases, the identification of alteration mineral zones has been used as proxies for uranium ore.

In addition, recent developments in the synthesis of uraniferous minerals (Clavier et al., 2014; Mesbah et al., 2015) and in Vis-NIR spectroscopy (Baron et al., 2014) have showed that this field technique

* Corresponding author.
E-mail address: valentin.robin@unilim.fr (V. Robin).

https://doi.org/10.1016/j.gexplo.2019.01.003
Received 26 October 2017; Received in revised form 14 January 2019; Accepted 15 January 2019
Available online 17 January 2019
0375-6742/

is an efficient tool to identify minor amounts of uranium bearing minerals within the coffinite-uranothorite series in rocks surrounding uranium deposits. Moreover, the determination of a spectral feature, which i) did not interfere with any other Vis-NIR bands of most rock-forming minerals that occur with coffinite, and ii) remains unaffected by compositional variation of the coffinite-thorite solid solution series (Baron et al., 2014), offers new opportunities for a quantitative approach (Andrews et al., 2017).

The goal of this study is to use the 1135 nm absorption band area in order to: i) determine the detection limit of coffinite in artificial sands made of mixtures of known proportions of quartz and synthetic coffinite (which simulate the sandy formations hosting the uranium within the roll-front); ii) determine a regression equation between the area of the 1135 nm absorption band and the amount of synthetic coffinite mixed with quartz in sands mixtures; iii) use this linear regression equation as a reference to quantify natural coffinite abundances in a set of mineralized samples of the Tortkuduk uranium roll-front deposit (South Kazakhstan); and iv) discuss the validity of the obtained quantification method using the mineralogical data of the Tortkuduk uranium ore deposit.

2. Geological context

The Tortkuduk uranium roll-front deposit belongs to the Muyunkum mining district, one of the major uranium deposits of the Shu Saryssu basin located in the South Kazakhstan (Yazikov, 2002; Dahlkamp, 2013). Such uranium deposits are characterized by low-grade and high tonnage reduced uranium mineralization hosted in roughly consolidated sand or sandstones. Roll-front deposits are typically divided in two compartments named after the redox condition prevailing in the sandy formations. Mineralization occurs at the redox front whereas reduced compartments are located ahead of uranium mineralization. Oxidized compartments are located behind and are typically depleted in uranium as the redox front progresses toward reduced formations. Information on both the geology and the mineralogical characteristics of the sandy formation hosting the roll-front uranium deposits of Tortkuduk are reported in Ben Simon (2009), Munara (2012), Dahlkamp (2013), Mathieu et al. (2015) or Robin et al. (2015). According to these authors, Tortkuduk uranium mineralization is dominated by very fine-grained coffinite minerals (< 1 μm) associated with sulphides (*e.g.* pyrite, marcasite) and organic matter. The uranium mineralization is hosted in a thick middle Eocene sand reservoir composed of sand channel accumulations in a coastal environment. The sandy formations constitute the reservoir. They vary from a relatively simple arenitic to arkosic mineralogical composition. Most of the uranium mineralization is hosted in fine-grained to very coarse-grained horizons of unconsolidated and highly permeable sands.

3. Materials and methods

3.1. Natural sands from the Tortkuduk uranium roll-front deposit

A total of 37 representative mineralized sand samples were collected from 14 drill-cores which intersected the sandy reservoir of the Tortkuduk deposit. The uranium content measured by X-ray fluorescence (XRF) ranges from 200 to 6200 ppm.

The average mineralogy of the selected samples comprise 65 to 74 wt% quartz, 9.5 to 19 wt% alkali feldspars (*e.g.* microcline and minor albite), 5 wt% micas (*e.g.* muscovite, biotite), 5 to 9 wt% clay minerals (*e.g.* smectite and kaolinite) and < 1 wt% accessory minerals which include coffinite, pyrite, marcasite, anatase, tourmaline, ilmenite, zircon and calcite (Ben Simon, 2009; Mathieu et al., 2015; Robin et al., 2015). Minor gypsum and goethite also occur in the oxidized compartments of the roll-front deposits (Munara, 2012). According to their grain size, these sands range from fine to medium-grained (*i.e.* 125 to 500 μm). The mean chemical analysis of a representative column of mineralized sand from this reservoir has been determined as follows: 87.07 wt% SiO_2; 5.97 wt% Al_2O_3; 1.28 wt% Fe_2O_3; 0.15 wt% FeO; 0.01 wt% MnO; 0.26 wt% MgO; 0.23 wt% CaO; 0.56 wt% Na_2O; 1.45 wt % K_2O; 0.20 wt% TiO_2; 0.10 wt% P_2O_5; 0.18 wt% U; 0.23 wt% S (Ben Simon, 2009).

Coffinite is the most common type of uranium-bearing mineral in all the samples (Boulesteix et al., 2015, Lach et al., 2015, Mathieu et al., 2015, Robin, 2015). Uraninite (pitchblende) and uranium-bearing alteration products of primary titaniferous minerals locally complete the uranium mineralization (Mathieu et al., 2015). Coffinite was only identified in the highly mineralized samples using X-ray diffraction (XRD) (Robin, 2015), whereas it was detected in each sample by scanning electron microscope observations coupled with energy dispersive X-ray analyses (SEM/EDS) (Boulesteix et al., 2015; Lach et al., 2015; Mathieu et al., 2015; Robin, 2015).

3.2. X-Rays fluorescence measurements

Chemical measurements were provided by the mining company, KATCO. The uranium content of natural sands was measured using the Innov-X Omega hand held XRF analyzer manufactured by Innov-X-Systems. The XRF readings were conducted in soil mode (*i.e.* a two-beam mode employing an internal Compton Normalization calibration). Each analysis lasted 4 min in total with 150 s using beam 1 conditions (heavy elements) and 90 s using beam 2 (light and transition elements).

3.3. Mineralogical sand mixtures

The sand mixtures consist of known amounts of quartz and coffinite and were designed to simulate arenitic sands containing from 0.005 wt % up to 1 wt% of coffinite in addition to quartz. To remain close to the field conditions, the sand mixtures were not ground at any stage of the preparation.

The source of quartz for the preparation of the sand mixtures was Fontainebleau sand NE34, a fine-grained natural arenitic sand (< 250 μm) containing > 98 wt% SiO_2 (Delfosse-Ribay et al., 2004).

A purified synthetic coffinite with a chemical composition of the ideal, end-member coffinite ($USiO_4$) was provided by the Institute for Chemical Separation of Marcoule (ICSM, France) for the preparation of sand mixtures. It consists of purified and well characterized aggregates of individual 80 nm-long crystals having the zircon structure type (tetragonal, $I4_1/amd$) (Mesbah et al., 2015; Szenknect et al., 2016). In natural samples of the Tortkuduk uranium roll-front deposit, coffinite also consists of very fine-grained particles (*i.e.* < 1 μm).

Eight mixtures of coffinite sands were prepared for this study: seven of which had a total mass of 2.5 g and a coffinite proportion of 1, 0.75, 0.5, 0.25, 0.1, 0.05, and 0.03 wt% respectively; and one with a total mass of 20 g and a coffinite proportion of 0.005 wt%. The proportion of Fontainebleau sand used for the mixtures corresponds to the difference between the total mass and the coffinite proportion. The uranium content for each sand mixture was calculated based on the wt% of purified coffinite in each sample (Table 1).

The control of the sample homogeneity was decisive considering the very low amounts of coffinite added to the Fontainebleau sand for the preparation of the sand mixtures. The obtained reflectance data in the Vis-NIR domain, which were collected from a surface analysis, are representative of the whole sample only if the three-dimensional homogeneity of the sample is verified. The small crystal size of the synthetic coffinite facilitated its dissemination in the quartz grain material even with very low coffinite amounts. The mixtures were made by slowly stirring the vials (30 rpm) for 2 days prior to the analysis. Special attention was paid to the handling of the sand mixtures to prevent them from shaking, in order to limit the settling of coffinite grains toward the bottom of the vials due to the high density of coffinite crystals ($d = 5.1\ g/cm^3$).

Table 1
Composition of sand mixtures and their calculated uranium content.

Sample	Fontainebleau sand (mg)	Coffinite (mg)	Coffinite (wt%)	Uranium (ppm)
SF-Co_0.005	19,999.00	1.00	0.005	36
SF-Co_0.03	2499.25	0.75	0.030	216
SF-Co_0.05	2498.75	1.25	0.050	360
SF-Co_0.10	2497.50	2.50	0.100	720
SF-Co_0.25	2493.75	6.25	0.250	1800
SF-Co_0.50	2487.50	12.50	0.500	3600
SF-Co_0.75	2481.25	18.75	0.750	5400
SF-Co_1.00	2475.00	25.00	1.000	7200

3.4. Reflectance measurements

The reflectance spectra were acquired using the ASD TerraSpec® 4 Standard-Res field spectrometer and the Indico® Pro software. The spectrometer includes: i) a fixed diffraction grating silicon (Si) array for the 350 to 1000 nm spectral region, and ii) two oscillating diffraction grating monochromators with cooled single element indium gallium arsenide (InGaAs) detectors for the 1000 to 2500 nm spectral region.

The spectral resolution of the detectors is 3 nm in the 350–1000 nm range and 10 nm in the 1000–2500 nm range. A contact probe that contains both the artificial lighting source (*e.g.* halogen lamp) and the optic fiber was used to analyze the samples.

The spectrometer and the contact probe were switched on 30 min prior the calibration and the acquisitions to ensure the stabilization of both the detectors and the halogen lamp. Each sample spectrum corresponds to the average of 50 stacked spectra acquired in about 7 s.

The samples were analyzed in two IR-transparent sample holders: i) sampling trays from the ASD Muglight accessory and ii) small glass vials. Natural samples were also introduced into the sample trays and measured without any preparation, as it is done in the field. The sand mixtures were prepared and analyzed in the same vials. Reproducibility tests were performed to ensure the homogeneity of the sand mixtures. The final Vis-NIR spectrum of each sample was the average of six individual measurements, whereby the vial was turned over between each reading to rearrange the sand mixtures. The number of six measurements was chosen as the addition of more spectra does not impact significantly the final averaged spectrum (from experiment). The high reproducibility of the Vis-NIR acquisitions validates the preparation procedure of the prepared sands. The Spectral Geologist™ (TSG™) software developed by the CSIRO was used in this study to visualize and analyze the spectral signature of samples.

4. Results and discussion

4.1. Vis-NIR reflectance spectra of sand mixtures

The Vis-NIR spectrum of the synthetic coffinite in sand mixtures is characterized by a series of absorptions bands at 1135 nm, 1418 nm, 1511 nm, 1678 nm and 2130 nm (Fig. 1A). The absorption features occurring under 1800 nm are attributed to the electronic transitions of the U^{4+} in the octahedral position of minerals with a zircon-type crystal structure (*e.g.* zircon ($ZrSiO_4$), thorite ($ThSiO_4$), coffinite ($USiO_4$)) and minerals of the thorite–coffinite solid solution series reported as uranothorite (Mackey et al., 1975; Zhang et al., 2003, 2009; Baron et al., 2014). To our knowledge, the multiple unusual sharp features observed between 350 and 700 nm are not described in the literature.

Quartz is a spectrally transparent mineral in the Vis-NIR spectral range (Hunt and Salisbury, 1970). However, spectra of pure Fontainebleau sand revealed the presence of weak absorption bands at 1418 nm, 1912 nm and 2208 nm (Fig. 1B). These features are due to very small amounts of phyllosilicates (< 0.1 wt%) within the quartz grains (French and Worden, 2013). These bands are attributed to the combination modes of OH vibrations of water molecules at 1912 nm (Madejová et al., 2009) and to the first overtone and the combination modes of OH vibrations of phyllosilicates near 1418 nm and 2208 nm, respectively (Post and Crawford, 2014).

4.2. Quantification of coffinite in sand mixtures

The diagnostic absorption features of coffinite (*i.e.* 660 nm, 1135 nm, 1418 nm, 1511 nm, 1678 nm and 2130 nm absorption bands described in Fig. 1) are observed in the Vis-NIR spectra of 8 sand mixtures in which the proportion of this mineral varies from 0.005 to 1 wt% (Fig. 2).

Coffinite can be detected in the reflectance spectrum of the sand mixtures from 0.005 wt%. For low coffinite contents, two features can be observed in the spectra at 660 nm and 1135 nm. The continuum removed

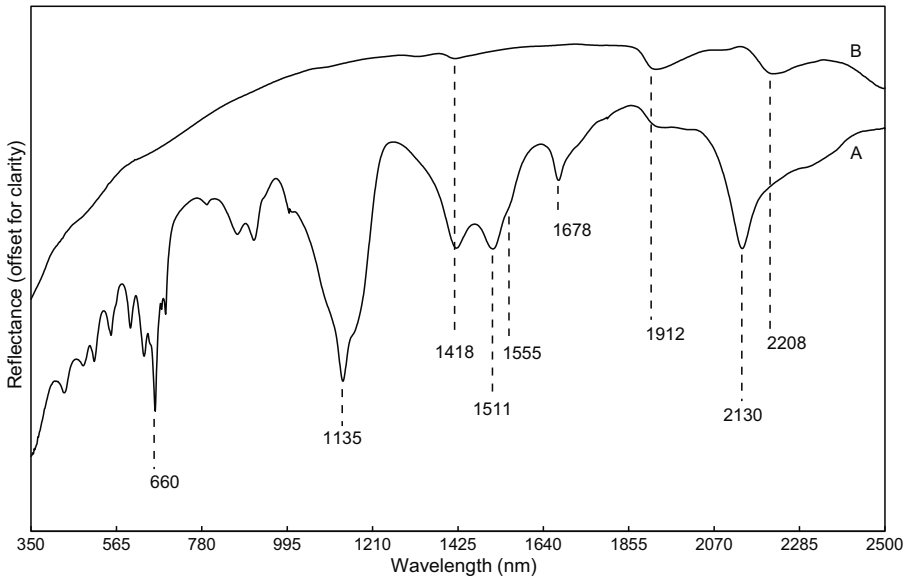

Fig. 1. Vis-NIR reflectance spectra of both pure coffinite (A) and Fontainebleau sand (B) samples. The vertical dashed lines show the wavelength position of the major absorption features and are discussed in the text.

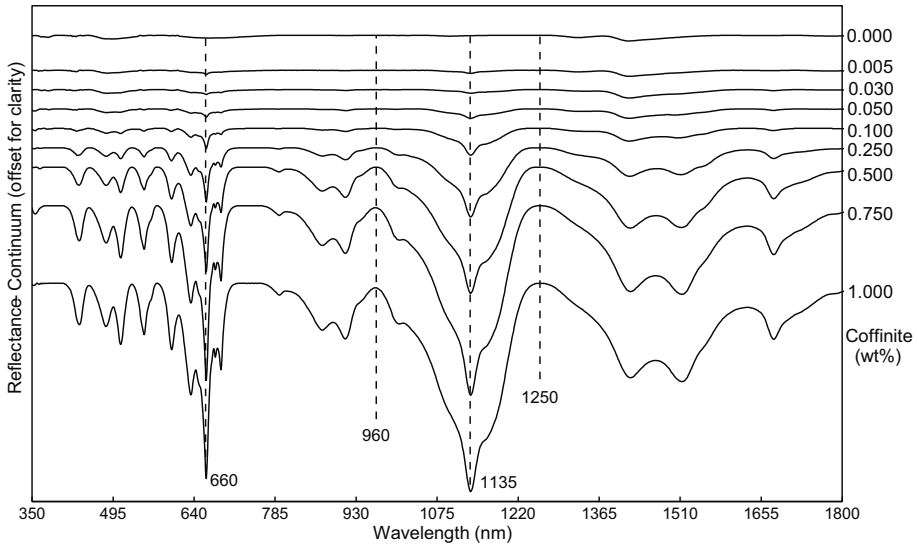

Fig. 2. Vis-NIR reflectance spectra of the sand mixtures. Continuum removal has been applied to enhance differences in shape between spectra. The coffinite content is indicated in the side of each sample spectrum. The vertical dashed lines indicate the wavelength range used to integrate the area of the 1135 nm band.

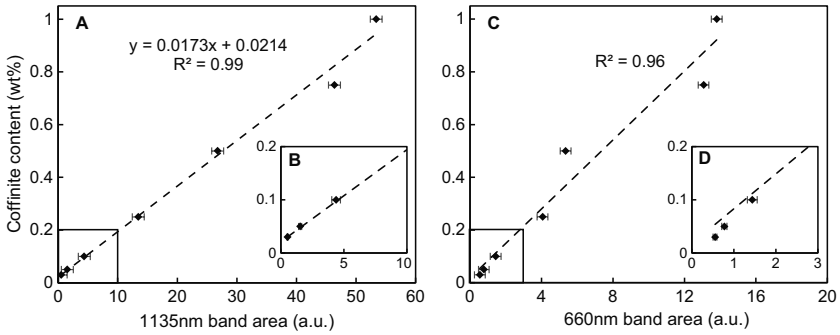

Fig. 3. Linear regressions between the integrated area of the 1135 nm band, the 660 nm band and the coffinite content of the sand mixtures.

spectra enhance the identification of these two spectral features in Fig. 2, in particular for coffinite contents of 0.005 and 0.03 wt%.

Under TSG™ software two specific spectral parameters (or scalars) were created to quantify the amount of coffinite from the 1135 nm and the 660 nm absorption bands.

Parameters were defined by isolating these bands from the overall shape of the spectrum using the standard "continuum removal" (Clark and Roush, 1984), also referred as "hull quotient" in TSG™. Relative absorption areas were integrated from: i) 960 nm to 1250 nm (*i.e.* the center wavelength was set to 1105 nm and the search radius to 145 nm) and ii) from 575 nm to 750 nm, for the 1135 nm and the 660 nm features respectively.

Fig. 3A and C shows positive linear correlations between the coffinite content and the 1135 nm and the 660 nm band area. The absorption feature at 1135 nm can be observed unambiguously with coffinite contents of 0.05 wt% or higher in sand mixtures (Fig. 3B). A positive linear correlation between the 660 nm and the 1135 nm band areas is logically deduced as the coffinite content increase in the sand mixtures. Both bands could be used as a spectral parameter to estimate the coffinite amount. However, for the same coffinite content, the 1135 nm band absorbs more than the 660 nm band. Natural sands usually contain a low coffinite amount; therefore, it is imperative to use the band that shows the highest absorption for coffinite content estimations. The average 1135 nm area (arbitrary unit, a.u.) and the standard deviation calculated for 6 individual spectral readings per sample are synthetized in Table 2.

The main factor of uncertainty for this method is due to the surface of the band, that lightly differs between the spectral readings conducted on the same sample. However, their standard deviation results showed an average area error of ± 8% arbitrary units. Such low variations will not have a significant impact on its ability to estimate the coffinite content using Vis-NIR spectra.

Unlike the absorption bands near 1420 nm, the 1135 nm feature of coffinite does not interfere with any other band of a mineral occurring in natural sands (*e.g.* phyllosilicates features observed in Fig. 4) and is a reliable marker of the coffinite content in the mineral mixtures. According to the Beer-Lambert law, the absorbance of a chemical bond is linearly related to its concentration in the structure of minerals composing a sample (Dahm and Dahm, 2001). The use of diffuse reflectance spectrometers, such as the TerraSpec® 4 Standard-Res, may give rise to a non-linearity of the absorbance-concentration relation due to scattering effects (Gobrecht et al., 2015).

The 1135 nm integrated area values for the sand mixtures containing 0.005 and 0.03 wt% coffinite using the aforementioned method are significantly higher than that measured for the pure Fontainebleau sand. However, the difference between the two values obtained for sand mixtures containing 0.005 and 0.03 wt% coffinite are not significantly different (Table 2). Such results suggest that coffinite can be detected but not quantified with the TerraSpec® 4 Standard-Res spectrometer when its content in the sand mixture is lower than 0.03 wt%.

For higher coffinite contents (*i.e.* from 0.03 to 1 wt%), the area of the 1135 nm band (x) increases with the coffinite wt% following a linear regression equation (see Eq. (1)) with a correlation coefficient equal to 0.99 (Fig. 3A).

Table 2
Integrated area of the 1135 nm band calculated with the TSG software and calculated uranium content from stoichiometry for sand mixtures.

Sample	Average area 1135 nm (a.u.)	Standard deviation	Coffinite (wt %)	Uranium (ppm)
Pure sand	0.07	0.03	0.000	0
SF-Co_0.005	0.47	0.05	0.005	36
SF-Co_0.03	0.52	0.07	0.030	216
SF-Co_0.05	1.53	0.20	0.050	360
SF-Co_0.10	4.38	0.08	0.100	720
SF-Co_0.25	13.45	1.13	0.250	1800
SF-Co_0.50	26.77	2.76	0.500	3600
SF-Co_0.75	46.38	1.19	0.750	5400
SF-Co_1.00	53.39	0.92	1.000	7200

$$\text{Coffinite wt\%} = 0.0173x + 0.0214 \quad (1)$$

In summary, if such an empirical relationship is applied to an arenitic sand analogue, coffinite should be detected at concentrations as low as 0.005 wt%. Coffinite would be accurately quantified between 0.03 and 1 wt% using the integrated area of the absorption band at 1135 nm.

4.3. Quantification of coffinite in natural sands: application to the Tortkuduk uranium roll-front deposit

The uranium content of the 37 mineralized samples from the Tortkuduk deposit, that were measured by XRF, vary in the same range than for the sand mixtures that were investigated in the previous section (*i.e.* from 200 to 6200 ppm and from 0 to 7200 ppm, respectively). The Vis-NIR spectra of 8 mineralized sand samples are characterized by several coffinite and phyllosilicate overlapping absorption features. The phyllosilicates consist of kaolinite, muscovite and smectite (Robin et al., 2015; Hebert et al., 2015) and their Vis-NIR spectra exhibit strong absorption bands near 1418 nm, 1912 nm and 2208 nm and partially interfere with the diagnostic bands of coffinite at 1418 nm, 1511 nm and 2130 nm.

Note that substantial amounts of alkali feldspar (mostly microcline) can be encountered in natural arkosic sands. Although these minerals can exhibit a weak absorption feature at 1210 nm due to the presence of Fe^{2+} in their structure (Anbalagan et al., 2009), this feature does not overlap with the specific coffinite absorption band at 1135 nm.

The use of this methodology could be limited due to the partial overlap of the 1135 nm feature of coffinite with broader absorption bands (centered between 350 and 1000 nm) related to electronic transitions in ferric iron oxide and hydroxide minerals such as hematite, or goethite (Ramanaidou et al., 2015). However, the local association of hematite or goethite with coffinite is unexpected in natural sands due to their stability at very different redox conditions (U^{4+} being oxidized into U^{6+} by Fe^{3+}). Coffinite crystallizes in reducing conditions and does not co-exist with hematite or goethite when oxidizing conditions prevail. In the Tortkuduk uranium deposit coffinite is restricted to the reduced section of the roll-front, whereas hematite or goethite are identified in the absence of coffinite within the oxidized compartment, where coffinite would dissolve and U^{6+} remobilized by the oxidizing solution (Szenknect et al., 2016).

Such results demonstrate that the 1135 nm feature observed on natural mineralized sand spectra appears to be the best candidate to quantify coffinite using Vis-NIR spectroscopy.

The coffinite content on Tortkuduk samples was determined empirically using Eq. (1) (established from the sand mixtures) and the 1135 nm band area calculated from the mineralized sand spectra. Fig. 5 shows the comparison between the uranium content calculated from the resulting coffinite content and the bulk uranium content of natural sands measured by XRF for each sample. Error bars represent the average standard deviation (4%) of band area that was calculated from each of the 37 natural sample Vis-NIR spectra.

Three main observations can be made based on the data presented Fig. 5:

1) For a majority of samples (*i.e.* 24 over 37), the uranium content attributed to the coffinite using the quantitative method based on IR spectroscopy does not deviate significantly from the total uranium content measured by XRF in natural sands. This is particularly true for the mineralized samples in which the total uranium content does not exceed 2000 ppm.
2) According to the fact that the uncertainties in the quantification methods are not strictly controlled, there is no case in which the uranium content in coffinite exceeds significantly (*i.e.* overestimate by > 1000 ppm of uranium) the total uranium content measured in the natural samples.

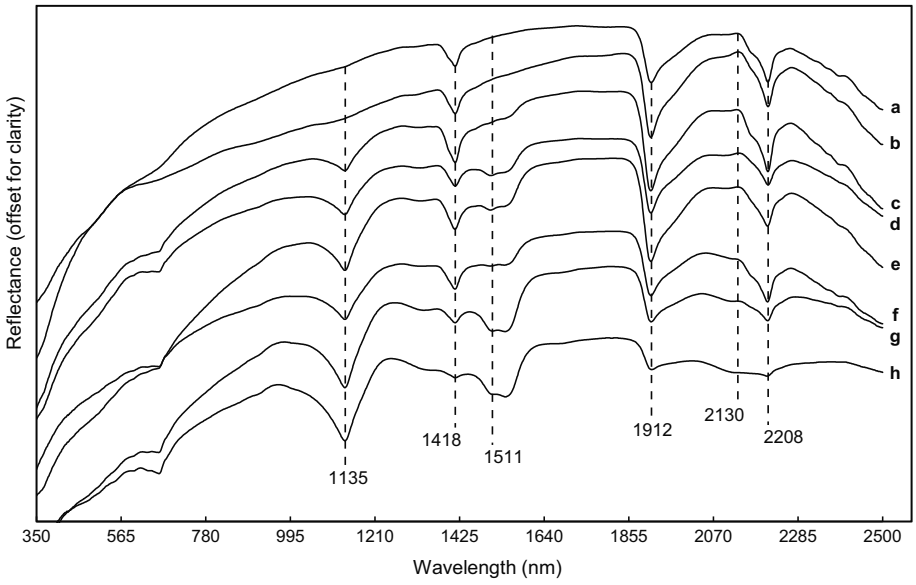

Fig. 4. Vis-NIR reflectance spectra of representative mineralized samples from the Tortkuduk roll-front uranium deposit. The vertical lines show the wavelength position of the major absorption features and are discussed in the text.

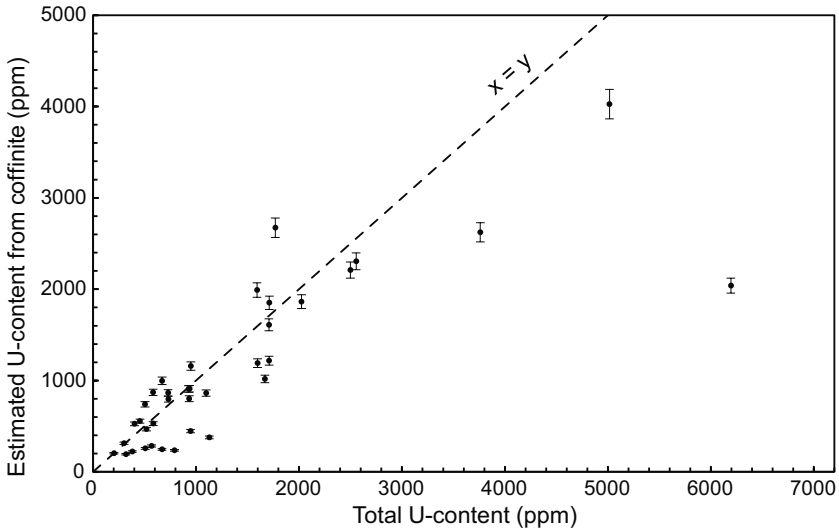

Fig. 5. Comparison of the total uranium content measured by XRF to the estimated uranium content contained in coffinite only. The dashed line represents the theoretical regression line for which the total uranium content is incorporated as U^{4+} in coffinite ($USiO_4$).

3) Conversely, several samples exhibited a content of uranium in coffinite significantly lower than the total uranium content on natural samples. This seems particularly the case for highest uranium grade samples (*i.e.* 5000 < uranium < 6200 ppm).

The quantitative results obtained in this study from Vis-NIR spectroscopy are consistent with the mineralogical characteristics of the mineralization encountered in the Tortkuduk uranium roll-front deposit (Boulesteix et al., 2015; Mathieu et al., 2015). The good correlation that exists between coffinite and the total uranium content of many natural sands agrees with the identification of coffinite as being the most common uranium bearing mineral type within the deposit (Mathieu et al., 2015).

For several samples and particularly for high-grade mineralization, the lowest uranium content found in coffinite compared to the total uranium content of the sand could be explained by the presence of additional uranium bearing minerals, such as primary titaniferous minerals and/or uraninite (pitchblende) that have been identified at the core of the uranium mineralized bodies (Mathieu et al., 2015). Unfortunately, uraninite (pitchblende) only show broad, low intensity features in the 350 to 2500 nm range investigated by Vis-NIR portable field spectrometers (Klunder et al., 2013).

Beside of the impact of additional uranium bearing mineral phases on the bulk uranium content present in sands, it cannot be excluded that part of the coffinite, previously formed in the mineralized zones, is now too amorphized to be fully identified by the Vis-NIR spectroscopy. Self-irradiation related to uranium decay in radioactive minerals (emission of alpha particles and their recoil effect) is known to damage the structure up to reach an amorphous state (metamict state) with increasing time (Ewing, 1994; Nasdala et al., 2005). Infrared studies on the reverse process of reconstructing zircon from an initial amorphous state showed an increase of intensity and complexity of the IR spectrum (Geisler et al., 2003). Consequently, naturally occurring coffinite may have a reduced number of configurations that can absorb in the Vis-NIR domain, lowering the level of available spectral information. The potential impact of metamictisation on the quantification of coffinite is supported by the $^{207}Pb/^{235}U$ ages of 2 to 20 My, which have been obtained for the mineralization of the Tortkuduk uranium roll-front deposits (Mathieu et al., 2015).

The above considerations support in the robustness of the method to quantify coffinite in roll-front uranium deposits, which use the 1135 nm feature as a relevant spectral parameter.

5. Conclusions

The present study proposed a new methodology to quantify coffinite ($USiO_4$) abundance in arenitic to arkosic sands or sandstones associated with roll-front uranium deposit using Vis-NIR portable field spectroscopy.

Previous works identified a diagnostic feature in the Vis-NIR spectra of coffinite at 1135 nm allowing a fast and convenient method to identify this mineral in complex mineralogical mixtures of altered granite (Baron et al., 2014). This feature presents several advantages: i) it does not interfere with any other Vis-NIR features of ubiquitous silicate minerals such as phyllosilicates (clay minerals particularly), and ii) results from electronic transitions of the U^{4+} cations in minerals with a zircon-type structure (Baron et al., 2014).

The coffinite content was determined using the 1135 nm feature measured from spectra acquired on a series of sand mixtures of arenitic sand and purified synthetic coffinite. The high correlation established between 1135 nm integrated area and the amount of coffinite in the sand mixtures shows that this mineral can be accurately quantified for concentrations between 0.03 and 1.0 wt%. The detection limit is 0.005 wt% and it is consistent with the concentrations encountered in the Torkuduk uranium roll-front deposit. Note that such a threshold is significantly lower than the one determined by Andrews et al. (2017) from Vis-NIR spectra of complex mineral mixtures prepared to simulate a metasomatic albitite uranium deposit of Australia.

The present methodology was then tested on natural samples from the Tortkuduk uranium roll-front deposit. The results confirm that coffinite is the main uranium-bearing mineral in most of the bulk samples uranium except in the higher-grade mineralization where uraninite or uranium-bearing titaniferous minerals have been identified by previous mineralogical investigations (Mathieu et al., 2015). This study demonstrates the efficiency and the high sensitivity of the Vis-NIR spectroscopy for the detection and the quantification of coffinite in uranium bearing sand or sandstone deposits. However, further works is required to: i) improve the accuracy of the coffinite quantification at the Muyunkum mining district scale, and ii) apply the proposed methodology to other worldwide sand or sandstone uranium deposits.

First, the uncertainty of the quantitative results obtained for the samples of Tortkuduk could be improved by taking into account the grain size effect of other minerals (in particular quartz and alkali feldspars) on the absorbency of coffinite. An additional linear regression equation between at the 1135 nm integrated area and the coffinite

concentrations in sandy sediments for grain sizes ranging from fine to coarse is required.

As the detection limits varies with the mineral mixtures (Hauff, 2008), the quantification of coffinite in other worldwide sand or sandstone deposits requires the definition of specific linear regression equations built from mineral mixtures representative as much as possible of the mineralogy of the studied deposit.

Finally, even if the Vis-NIR spectroscopy is known as a suitable method to identify poorly organized crystalline structures (Hauff, 2008), experimental works would be necessary to determine the effects of metamictisation on the 1135 nm band area of coffinite encountered in natural uranium deposits.

Acknowledgements

The authors gratefully acknowledge R. Mathieu, M. Distinguin, Y. Deschamps, M. Brouand and the geology team from KATCO Inc. for their previous work on the subject and for providing advices, background, sample material, XRF analysis and logistic support as well as the chemistry team from the ICSM laboratory for providing the synthetic coffinite. This work has been financially supported by AREVA Mines and the NEEDS program.

References

Anbalagan, G., Sankari, G., Ponnusamy, S., kumar, R.T., Gunasekaran, S., 2009. Investigation of silicate mineral sanidine by vibrational and NMR spectroscopic methods. Spectrochim. Acta A Mol. Biomol. Spectrosc. 74, 404–409. https://doi.org/10.1016/j.saa.2009.06.034.

Andrews, W.L., Tardio, J., Bhargava, S.K., Wilde, A., Otto, A., Pownceby, M.I., 2017. Development of a new near infrared (NIR) tool for quantifying coffinite ($USiO_4$) in a moderately complex uranium ore analogue. J. Geochem. Explor. 182, 80–93. https://doi.org/10.1016/j.gexplo.2017.09.003.

Baron, F., Robin, V., Beaufort, D., Szenknect, S., Dacheux, N., Petit, S., 2014. Technical note: use of near infrared spectroscopy for the identification of coffinite and uranothorite. J. Infrared Spectrosc. 22, 149. https://doi.org/10.1255/jnirs.1110.

Ben Simon, R., 2009. Experimental Study and Numerical Modelling of Geochemical Reactions Occurring During Uranium In Situ Recovery (ISR) Mining. (PhD thesis).

Boulesteix, T., Cathelineau, M., Lach, P., Deloule, E., Brouand, M., Fiet, N., Toubon, H., 2015. Ilmenite and Their Alteration Products, Sinkholes for Uranium and Radium in Roll Front Deposits After the Example of South Tortkuduk (Kazakhstan). Presented at the 13th SGA Biennial Meeting, Nancy.

Clark, R.N., Roush, T.L., 1984. Reflectance spectroscopy: quantitative analysis techniques for remote sensing applications. J. Geophys. Res. Solid Earth 89, 6329–6340.

Clavier, N., Szenknect, S., Costin, D., Mesbah, A., Poinssot, C., Dacheux, N., 2014. From thorite to coffinite: a spectroscopic study of $Th_{1-x}U_xSiO_4$ solid solutions. Spectrochim. Acta A Mol. Biomol. Spectrosc. 118, 302–307.

Dahlkamp, F.J., 2013. Uranium Ore Deposits. Springer Science & Business Media.

Dahm, D.J., Dahm, K.D., 2001. The physics of near-infrared scattering. In: Near-Infrared Technol. Agric. Food Ind. 2.

Delfosse-Ribay, E., Djeran-Maigre, I., Cabrillac, R., Gouvenot, D., 2004. Shear modulus and damping ratio of grouted sand. Soil Dyn. Earthq. Eng. 24, 461–471. https://doi.org/10.1016/j.soildyn.2004.02.004.

Dill, H.G., 2016. Kaolin: soil, rock and ore: from the mineral to the magmatic, sedimentary and metamorphic environments. Earth Sci. Rev. 161, 16–129.

Ewing, R.C., 1994. The metamict state: 1993 — the centennial. Nucl. Instrum. Methods Phys. Res., Sect. B 91, 22–29. https://doi.org/10.1016/0168-583X(94)96186-7.

French, M.W., Worden, R.H., 2013. Orientation of microcrystalline quartz in the Fontainebleau Formation, Paris Basin and why it preserves porosity. Sediment. Geol. 284–285, 149–158. https://doi.org/10.1016/j.sedgeo.2012.12.004.

Geisler, T., Zhang, M., Salje, E.K.H., 2003. Recrystallization of almost fully amorphous zircon under hydrothermal conditions: an infrared spectroscopic study. J. Nucl. Mater. 320, 280–291. https://doi.org/10.1016/S0022-3115(03)00187-9.

Gobrecht, A., Bendoula, R., Roger, J.-M., Bellon-Maurel, V., 2015. Combining linear polarization spectroscopy and the Representative Layer Theory to measure the Beer–Lambert law absorbance of highly scattering materials. Anal. Chim. Acta 853, 486–494. https://doi.org/10.1016/j.aca.2014.10.014.

Hauff, P., 2008. An Overview of VIS-NIR-SWIR Field Spectroscopy as Applied to Precious Metals Exploration. 80001. Spectr. Int. Inc., pp. 303–403.

Hebert, B., Beaufort, D., Roy, R., Pouradier, A., Jikibayev, R., 2015. New Methods to Quantify Clay Minerals in the Uranium Deposits Hosted in Sands of the Chu Sarysu Basin (South Kazakhstan) Based on Visible and Near-Infrared Field Spectrometry.

Herrmann, W., Blake, M., Doyle, M., Huston, D., Kamprad, J., Merry, N., Pontual, S., 2001. Short wavelength infrared (SWIR) spectral analysis of hydrothermal alteration zones associated with base metal sulfide deposits at Rosebery and Western Tharsis, Tasmania, and Highway-Reward, Queensland. Econ. Geol. 96, 939–955.

Hunt, G.R., Ashley, R.P., 1979. Spectra of altered rocks in the visible and near infrared. Econ. Geol. 74, 1613–1629.

Hunt, G.R., Salisbury, J.W., 1970. Visible and near-infrared spectra of minerals and rocks: I silicate minerals. Mod. Geol. 1, 283–300.

Klunder, G.L., Plaue, J.W., Spackman, P.E., Grant, P.M., Lindvall, R.E., Hutcheon, I.D., 2013. Application of visible/near-infrared reflectance spectroscopy to uranium ore concentrates for nuclear forensic analysis and attribution. Appl. Spectrosc. 67, 1049–1056.

Kruse, F.A., Boardman, J.W., Huntington, J.F., 2003. Comparison of airborne hyperspectral data and eo-1 hyperion for mineral mapping. IEEE Trans. Geosci. Remote Sens. 41, 1388–1400. https://doi.org/10.1109/TGRS.2003.812908.

Lach, P., Cathelineau, M., Brouand, M., Fiet, N., 2015. In-situ isotopic and chemical study of pyrite from Chu-Sarysu (Kazakhstan) roll-front uranium deposit. Earth Planet. Sci. Lett. 13, 207–210. https://doi.org/10.1016/j.proeps.2015.07.049.

Mackey, D.J., Runciman, W.A., Vance, E.R., 1975. Crystal-field calculations for energy levels of U^{4+} in $ZrSiO_4$. Phys. Rev. B 11, 211–218. https://doi.org/10.1103/PhysRevB.11.211.

Madejová, J., Pentrák, M., Pálková, H., Komadel, P., 2009. Near-infrared spectroscopy: a powerful tool in studies of acid-treated clay minerals. Vib. Spectrosc. 49, 211–218. https://doi.org/10.1016/j.vibspec.2008.08.001.

Mathieu, R., Deschamps, Y., Selezneva, V., Pouradier, A., Brouand, M., Deloule, E., Boulesteix, T., 2015. Key Mineralogical Characteristics of the New South Tortkuduk Uranium Roll-front Deposits, Kazakhstan. Presented at the 13th SGA Biennial Meeting, Nancy.

Mathieu, M., Roy, R., Launeau, P., 2017. Alteration mapping on drill cores using a HySpex SWIR-320m hyperspectral camera: application to the exploration of an unconformity-related uranium deposit (Saskatchewan, Canada). J. Geochem. Explor. 172, 71–88.

Mesbah, A., Szenknect, S., Clavier, N., Lozano-Rodriguez, J., Poinssot, C., Den Auwer, C., Ewing, R.C., Dacheux, N., 2015. Coffinite, $USiO_4$, is abundant in nature: so why is it so difficult to synthesize? Inorg. Chem. 54, 6687–6696. https://doi.org/10.1021/ic502808n.

Munara, A., 2012. Formation des gisements d'uranium de type roll: approche minéralogique et géochimique du gisement uranifère de Muyunkum (Bassin de Chu-Sarysu, Kazakhstan). (PhD 327p).

Nasdala, L., Hanchar, J.M., Kronz, A., Whitehouse, M.J., 2005. Long-term stability of alpha particle damage in natural zircon. Chem. Geol. 220, 83–103. https://doi.org/10.1016/j.chemgeo.2005.03.012.

Pontual, S., Merry, N., Gamson, P., 1997. G-Mex Vol. 1, Spectral Interpretation Field Manual. Ausspec Int. Pty. Ltd., Kew Vic, pp. 3101.

Post, J.L., Crawford, S.M., 2014. Uses of near-infared spectra for the identification of clay minerals. Appl. Clay Sci. 95, 383–387. https://doi.org/10.1016/j.clay.2014.02.010.

Ramanaidou, E., Wells, M., Lau, I., Laukamp, C., 2015. Characterization of iron ore by visible and infrared reflectance and, Raman spectroscopies. In: Iron Ore: Mineralogy, Processing and Environmental Sustainability. Woodhead Publishing, pp. 191–228.

Robin, V., 2015. Effet de la cristallochimie des minéraux argileux gonflants sur les propriétés d'échange cationique et de dissolution. Implications dans un contexte de réhabilitation de sites miniers acidifiés. (PhD 190p).

Robin, V., Hebert, B., Beaufort, D., Sardini, P., Tertre, E., Regnault, O., Descostes, M., 2015. Occurrence of authigenic beidellite in the Eocene transitional sandy sediments of the Chu-Saryssu basin (South-Central Kazakhstan). Sediment. Geol. 321, 39–48. https://doi.org/10.1016/j.sedgeo.2015.03.004.

Szenknect, S., Mesbah, A., Cordara, T., Clavier, N., Brau, H.-P., Le Goff, X., Poinssot, C., Ewing, R.C., Dacheux, N., 2016. First experimental determination of the solubility constant of coffinite. Geochim. Cosmochim. Acta 181, 36–53. https://doi.org/10.1016/j.gca.2016.02.010.

Xu, Q.-J., Ye, F.-W., Liu, S.-F., Zhang, Z.-X., Zhang, C., 2017. Hyperspectral alteration information from drill cores and deep uranium exploration in the Baiyanghe uranium deposit in the Xuemisitan area, Xinjiang, China. Remote Sens. 9, 451. https://doi.org/10.3390/rs9050451.

Yazikov, V., 2002. Uranium raw material base of the Republic of Kazakhstan and prospects of using in situ leach mining for its development. In: Situ Leach Uranium Min. T1-TC-975 IAEA Vienna 22–31.

Zhang, M., Salje, E.K., Ewing, R.C., 2003. Oxidation state of uranium in metamict and annealed zircon: near-infrared spectroscopic quantitative analysis. J. Phys. Condens. Matter 15, 3445.

Zhang, F.X., Pointeau, V., Shuller, L.C., Reaman, D.M., Lang, M., Liu, Z., Hu, J., Panero, W.R., Becker, U., Poinssot, C., Ewing, R.C., 2009. Structural transitions and electron transfer in coffinite, $USiO_4$, at high pressure. Am. Mineral. 94, 916–920. https://doi.org/10.2138/am.2009.3111.